The effect of pore fluid on the stress-dependent elastic wave velocities in sandstones

Colin M. Sayers, Schlumberger, and De-Hua Han, Houston Advanced Research Center*

Summary

Elastic wave velocities in sandstones vary with stress due to the presence of discontinuities such as grain boundaries and microcracks within the rock. The effect of any discontinuities on the elastic wave velocities can be written in terms of a second-rank and fourth-rank tensor that quantify the dependence of the elastic wave velocities on the orientation distribution and normal and shear compliances of the discontinuities. This allows the normal and shear compliance of these discontinuities to be obtained as a function of stress by inverting measurements of *P*- and *S*-wave velocities. Inversion of ultrasonic velocity measurements on dry and fluid saturated sandstones shows that the ratio of the normal to shear compliance of the discontinuities is reduced in the presence of fluid in the grain boundaries and microcracks. This is consistent with the expected reduction in the normal compliance of the discontinuities in the presence of a fluid with non-zero bulk modulus.

Introduction

Gassmann's equations (Gassmann, 1951) relate the low frequency bulk modulus, K_{sat}, and shear modulus, μ_{sat}, of a fluid saturated porous rock to the bulk modulus, K_{frame}, and shear modulus, μ_{frame}, of the rock frame without fluid in the pores. These equations may be written in the form:

$$K_{sat} = K_{frame} + \frac{(1 - K_{frame}/K_0)^2}{(f/K_{fl} + (1-f)/K_0 - K_{frame}/K_0^2)} \quad (1)$$

$$m_{sat} = m_{dry} \quad (2)$$

Here K_0 is the bulk modulus of the solid material making up the rock frame, K_{fl} is the bulk modulus of the fluid, and ϕ is the porosity (see, for example, Mavko et al., 1998). It should be noted that the frame moduli, K_{frame}, and μ_{frame}, used to predict the low frequency elastic moduli in fluid saturated porous rocks, correspond to the moduli of the frame in contact with a small amount of residual fluid. Drying the rock in an oven, for example, can alter the physical properties of clay and disrupt the surface forces acting at the surface of the grains.

In sandstones, the frame moduli, K_{frame} and μ_{frame}, vary strongly with stress due to the presence of discontinuities within the rock such as boundaries between sand grains and microcracks, as illustrated in Figure 1. Figure 2 shows the variation of K_{sat}/K_0 as a function of K_{frame}/K_0, for a sandstone having the properties ϕ=0.2, K_0=36 GPa, saturated with a fluid having bulk modulus K_{fl}=2.2 GPa. K_{frame}/K_0 is expected to increase with increasing stress due to increasing contact between opposing faces of grain boundaries and microcracks. K_{sat}/K_0 is seen to increase at a lower rate, particularly at low stress.

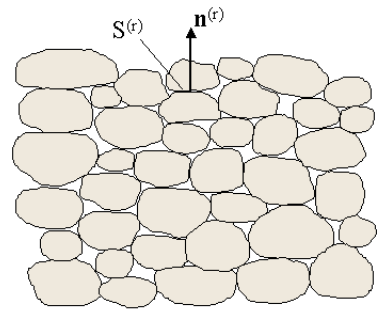

Figure 1 – A region within a sandstone showing the discontinuities between sand grains.

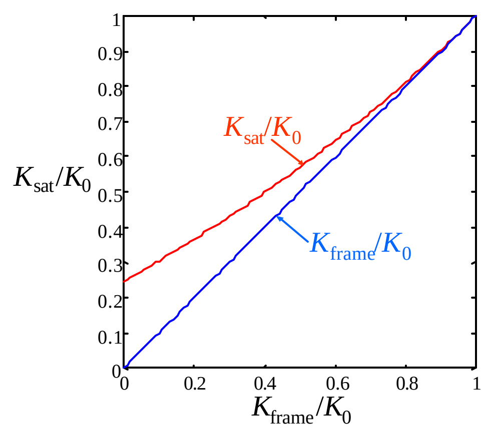

Figure 2 – Variation of K_{sat}/K_0 as a function of K_{frame}/K_0, for a sandstone having the properties ϕ=0.2, K_0=36 GPa, saturated with water having bulk modulus K_{fl}=2.2 GPa.

A further effect of fluid on the stress-dependence of elastic wave velocities in sandstones results from the breakdown of the low frequency assumption implicit in Gassmann's equations. As frequency increases, viscous effects cause the thinnest pores (microcracks and grain boundaries) to become isolated with respect to fluid flow (Mavko and Jizba, 1991, 1994). Because the pore pressure induced in these pores is unable to equilibriate with the pore pressure in the rest of the pore space, the rock frame appears stiffer than at lower frequencies. Mavko and Jizba (1991, 1994) consider the thin, compliant fraction of the pore space to be part of the viscoelastic frame of the rock, and derive equations for the high-frequency frame moduli that incorporate the stiffening effect of the fluid in the thin, compliant fraction of the pore space. These expressions may then be substituted into Gassmann's equations to incorporate the remaining fluid saturation effects. At finite frequencies, squirt flow occurs between the low aspect ratio pores and the rest of the pore space, resulting in a frequency dependent frame modulus. Murphy et al. (1984) introduced a micromechanical model to describe squirt flow at grain boundaries, consisting of the parallel combination of the stiffness of the grain contact and the stiffness of a fluid-filled gap. The purpose of this paper is to invert for the properties of fluid-filled grain boundaries and microcracks using *P*- and *S*-wave velocity measurements as a function of stress.

Theoretical model

It is assumed that the stress dependence of the elastic properties of a sandstone is due to deformation of any discontinuities within the rock such as microcracks and boundaries between sand grains. At high confining stress, any discontinuities are assumed to close so that the sandstone may be treated as an anisotropic elastic medium with elastic stiffness tensor C^0_{ijkl} and elastic compliance tensor S^0_{ijkl}. At intermediate stress it is assumed that any discontinuities will be partially open. Because the compliance of a discontinuity varies with stress, as more and more contacts are made between opposing faces of the discontinuity, elastic wave velocities in sedimentary rocks are strongly non-linear functions of stress.

Mavko et al. (1995) treat the stress-dependent wave velocities in the presence of discontinuities such as cracks and compliant grain boundaries by defining a fourth-rank compliance tensor for each discontinuity, and by summing the compliance tensors for all discontinuities. In this paper, the approach of Sayers and Kachanov (1991, 1995) is used in which the variation in elastic wave velocity resulting from the deformation of all such discontinuities is expressed in terms of a single second-rank and fourth-rank tensor. These tensors quantify the effect on the elastic wave velocities of the orientation distribution and normal and shear compliances of the grain boundaries and microcracks. The expressions given allow ultrasonic velocity measurements to be inverted to obtain the components of these tensors. These components represent the maximum information about the orientation distribution of the discontinuities that can be determined from elastic wave velocity measurements.

Following Sayers and Kachanov (1991, 1995), the elastic compliance of the sandstone frame may be written in the form

$$S_{ijkl} = S^0_{ijkl} + \Delta S_{ijkl} \,, \qquad (3)$$

where the excess compliance ΔS_{ijkl} due to the discontinuities can be written as

$$\Delta S_{ijkl} = \frac{1}{4}\left(\delta_{ik}\alpha_{jl} + \delta_{il}\alpha_{jk} + \delta_{jk}\alpha_{il} + \delta_{jl}\alpha_{ik}\right) + \beta_{ijkl} \qquad (4)$$

Here, α_{ij} is a second-rank tensor and β_{ijkl} is a fourth rank tensor defined by

$$\alpha_{ij} = \frac{1}{V}\sum_r B_T^{(r)} n_i^{(r)} n_j^{(r)} A^{(r)} \qquad (5)$$

$$\beta_{ijkl} = \frac{1}{V}\sum_r \left(B_N^{(r)} - B_T^{(r)}\right) n_i^{(r)} n_j^{(r)} n_k^{(r)} n_l^{(r)} A^{(r)} \qquad (6)$$

$B_N^{(r)}$ and $B_T^{(r)}$ are the normal and shear compliance of the *r*th discontinuity, $n_i^{(r)}$ is the *i*th component of the normal to the discontinuity, and $A^{(r)}$ is the area of the discontinuity (Sayers and Kachanov, 1991, 1995). $B_N^{(r)}$ characterizes the displacement jump normal to the discontinuity produced by a normal traction, while $B_T^{(r)}$ characterizes the shear displacement jump produced by a shear traction applied at the discontinuity. $B_T^{(r)}$ is assumed to be independent of the direction of the shear traction within the plane of the discontinuity. Note that α_{ij} and β_{ijkl} are symmetric with respect to all rearrangements of the indices so that, for example, $\beta_{1122}=\beta_{1212}$, $\beta_{1133}=\beta_{1313}$, etc. If $B_N=B_T$ for all discontinuities, the fourth-rank tensor β_{ijkl} vanishes and ΔS_{ijkl} is completely determined by the second-rank tensor α_{ij}.

Inversion of ultrasonic velocity measurements

The components α_{ij} and β_{ijkl} of the second and fourth rank tensors introduced above may be obtained from equation (3) by inverting elastic stiffnesses obtained from measured *P*- and *S*-wave velocities. Han (1986) and Han et al. (1986) report measurements of *P*- and *S*-wave velocities for a large number of dry and saturated sandstones as a function of applied hydrostatic stress. Because velocity measurements were only made in one direction, it is assumed below that the samples are isotropic. For isotropic sandstones subject to a hydrostatic stress state, it follows from equations (5) and (6) that the non-vanishing α_{ij} and β_{ijkl} are

$$\alpha_{11} = \alpha_{22} = \alpha_{33} = \alpha \text{ , say} \qquad (7)$$

$$\beta_{1111} = \beta_{2222} = \beta_{3333} = \beta \text{ , say} \qquad (8)$$

$$\beta_{1122} = \beta_{1133} = \beta_{2233} = \beta_{1212} = \beta_{1313} = \beta_{2323} = \beta/3 \qquad (9)$$

It then follows from equation (4) that the frame bulk modulus, K, and shear modulus, μ, are given in terms of the bulk modulus, K_0, and shear modulus, μ_0, of the frame at high confining stress by

$$K = \frac{K_0}{1+3K_0(\alpha+5\beta/3)}, \quad \mu = \frac{\mu_0}{1+2\mu_0(\alpha+2\beta/3)} \, . \quad (10)$$

These equations allow α and β to be determined from measurements of the *P*- and *S*-wave velocities using the relations

$$v_P = \sqrt{(K+4\mu/3)/\rho}\, , \quad v_S = \sqrt{\mu/\rho}\, , \qquad (11)$$

where ρ is the density.

Finally, consider a sandstone with an isotropic orientation distribution of discontinuities subject to a hydrostatic stress. Denoting the average normal and shear compliance by B_N and B_T, it follows from equations (5) and (6) that $B_N/B_T = 1+5\beta/3\alpha$. This allows B_N/B_T to be estimated from the ratio β/α.

Application to velocity measurements on sandstones

Han (1986) and Han et al. (1986) report measurements of *P*- and *S*-wave velocities on dry and saturated sandstone samples subject to a hydrostatic confining stress of 5, 10, 20, 30, 40 and 50 MPa. To determine α and β from equations (10-11), the bulk modulus, K_0, and shear modulus, μ_0, of the frame at high confining stress were estimated from the velocity measurements at the highest confining stress for which velocity measurements were made. The values of α and β found below therefore correspond to changes relative to this reference state of the rock.

To illustrate the results, Figure 3 shows the variation of the *P*- and *S*-wave velocity for one of the dry samples measured by Han (1986). It is seen that the velocities increase with increasing hydrostatic stress, as grain boundaries and microcracks within the rock close with increasing stress. Figure 3 also shows the variation of α and β versus stress for this rock. It is seen that the microcracks and grain boundaries become less compliant as the hydrostatic stress increases. This is consistent with the expectation that the compliance of the grain boundaries and microcracks decreases as the stress increases due to increasing contact between opposing faces of these discontinuities. It is also seen that, for this rock, α and β are of opposite sign. This implies that $B_N/B_T<1$ for this rock (see equations (5) and (6)). The discontinuities are therefore more compliant in shear than in compression, as found previously for Penrith sandstone (Sayers, 2002).

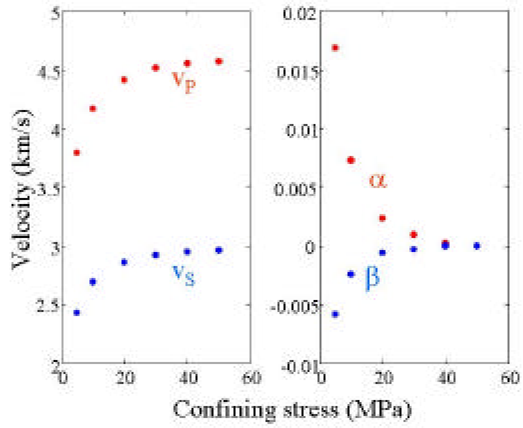

Figure 3 – Left: Variation of the P- and S-wave velocity versus confining stress for one of the dry samples measured by Han (1986). Right: Variation of α and β as a function of confining stress obtained using equations (10-11).

Figure 4 shows a histogram of B_N/B_T deduced for the dry samples measured by Han et al. (1986). It is seen that for most of these samples $B_N/B_T<1$. However an appreciable number of the samples have values of $B_N/B_T>1$.

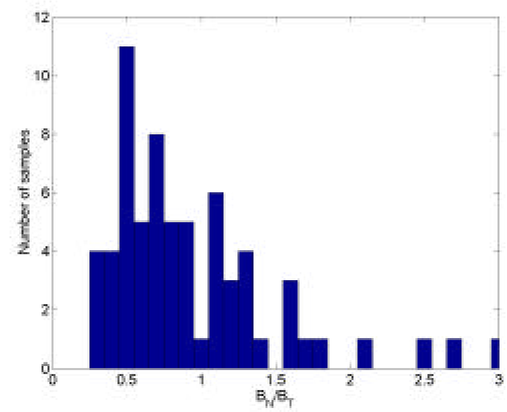

Figure 4 – Histogram of B_N/B_T obtained for the dry samples of Han (1986).

To determine B_N/B_T for the fluid saturated samples, it is necessary to determine the bulk and shear moduli of the frame. The shear modulus of the frame follows directly from equation (2), while the bulk modulus of the frame may be written as

$$K_{frame} = \frac{K_{sat}\left(\phi K_0/K_{fl} + 1 - \phi\right) - K_0}{\left(\phi K_0/K_{fl} + K_{sat}/K_0 - 1 - \phi\right)} \qquad (13)$$

(see, for example, Mavko et al., 1998).

Figure 5 shows a histogram of B_N/B_T for the saturated samples measured by Han (1986) obtained using the wet frame moduli calculated for these samples. It is seen that the presence of fluid in the grain boundaries and microcracks acts to decrease the ratio B_N/B_T from the values in dry sandstones (compare Figures 4 and 5). This implies that B_N/B_T is reduced due to the presence of fluid, consistent with the expected reduction in normal compliance for fluid-saturated microcracks and grain boundaries (Sayers, 1999). It is also seen that the distribution of B_N/B_T for fluid-saturated sandstones is much narrower than for dry sandstones (note the change in vertical scale between figures 4 and 5).

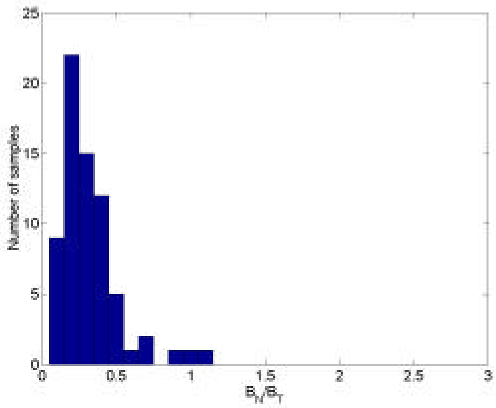

Figure 5 – Histogram of B_N/B_T obtained for the saturated samples of Han (1986).

Conclusion

A theory of the stress-dependent *P*- and *S*-wave velocities in dry and fluid-saturated sandstones has been presented that takes into account the deformation of discontinuities in the rock such as grain boundaries and microcracks. The theory is formulated in terms of a second-rank tensor, α_{ij}, and a fourth-rank tensor, β_{ijkl}, which depend on the orientation distribution and the normal and shear compliance of these discontinuities. The theory allows the components of these tensors to be obtained as a function of stress from measurements of *P*- and *S*-wave velocities. Application of the theory to the velocity measurements reported by Han (1986) and Han et al. (1986) on dry and saturated sandstones, shows that, for saturated samples, α and β are of opposite sign. The ratio B_N/B_T of the normal to shear compliance of the microcracks is therefore less than one for saturated sandstones, implying that the grain contacts and microcracks are more compliant in shear than in compression. For dry samples β/α is larger than for fluid-saturated samples. The ratio B_N/B_T of the normal to shear compliance of the microcracks and grain boundaries is therefore reduced in the presence of fluid, consistent with the expected reduction in normal compliance for fluid-saturated microcracks and grain boundaries.

Acknowledgment

We thank Boris Gurevich for helpful discussions.

References

Gassmann, F., 1951, Über die Elastizität poröser Medien, *Vier. der Natur. Gesellschaft in Zürich,* **96**, 1-23.

Han, D.-H., 1986, Effects of porosity and clay content on acoustic properties of sandstones and unconsolidated sediments, *Ph.D. Thesis,* Stanford Univ.

Han, D.-H., Nur, A., and Morgan, D., 1986, Effects of porosity and clay content on wave velocities in sandstones, *Geophysics*, **51**, 2093-2107.

Mavko, G., and Jizba, D., 1991, Estimating grain-scale fluid effects on velocity dispersion in rocks, *Geophysics*, **56**, 1940-1949.

Mavko, G., and Jizba, D., 1994, The relation between seismic P- and S-wave velocity dispersion in saturated rocks, *Geophysics*, **59**, 87-92.

Mavko, G., Mukerji, T., and Godfrey, N., 1995, Predicting stress-induced velocity anisotropy of rocks, *Geophysics*, **60**, 1081-1087.

Mavko, G., Mukerji, T., and Dvorkin, J., 1998, *The rock physics handbook*, Cambridge Univ. Press.

Murphy, W.F., Winkler, K.W., and Kleinberg, R.L., 1984, Contact microphysics and viscous relaxation in sandstones, in Johnson, D.L., and Sen, P.N., Eds. *Physics and Chemistry of Porous Media*, Am. Inst. Phys., 176-190.

Sayers, C.M., 1999, Stress-dependent seismic anisotropy of shales, *Geophysics*, **64**, 93-98.

Sayers, C.M., 2002, Stress-dependent elastic anisotropy of sandstones, *Geophys. Prosp.*, **50**, 85-95.

Sayers, C.M., and Kachanov, M., 1991, A simple technique for finding effective elastic constants of cracked solids for arbitrary crack orientation statistics, *Int. J. Solids Structures*, **12**, 81-97.

Sayers, C.M., and Kachanov, M., 1995, Microcrack-induced elastic wave anisotropy of brittle rocks, *J. Geophys. Res.*, **100**, 4149-4156.